

# T-Shaped MIMO Antenna Design with Defected Ground Structure and Parasitic Elements for 5G Application

## Perancangan Antena MIMO T-Shaped Dengan Defected Ground Structure Dan Elemen Parasitic Pada Aplikasi 5G

Ayu Mika Sherila<sup>\*1</sup>, Umaisaroh Umaisaroh<sup>2</sup>, Mudrik Alaydrus<sup>3</sup>

<sup>1</sup>*Teknik Elektro, Fakultas Teknik, Universitas Pembangunan Nasional Veteran Jakarta*

<sup>2,3</sup>*Teknik Elektro, Fakultas Teknik, Universitas Mercu Buana*

\*<sup>1</sup> Corresponding author: ayu.sherila@upnvj.ac.id

Received on 03-10-2024, accepted on 02-01-2025, published on 27-01-2025

### Abstract

5G technology is designed to improve efficiency, network capacity, data rate, and coverage with low power consumption. This requires the design of suitable antennas for 5G wireless communications to achieve optimal bandwidth, radiation, efficiency, and performance. MIMO antenna designs use multiple antennas and face the main challenge of reducing mutual coupling between adjacent antenna elements. In this study, the MIMO antenna is designed using T-shaped DGS Technique and parasitic elements. The DGS technique is developed by creating a specific area on the ground plane of the antenna to improve its performance. By incorporating DGS concepts and parasitic elements into the design, the aim is to achieve large bandwidth and high gain. This antenna has dimensions of 52 mm x 12 mm and is simulated using Ansys HFSS software. Measurement results for the antenna using Rogers Duroid RT5880 substrate show a mutual coupling value of -54.2 dB, return loss of -11.1 dB, gain of 13.11 dB, and a sufficiently wide bandwidth. Thus, the proposed antenna can operate at a frequency of 28 GHz, meeting the requirements for 5G applications.

**Keywords:** DGS, Parasitic Elements, MIMO, Mutual Coupling, 5G

### Abstrak

Teknologi 5G dirancang untuk meningkatkan efisiensi, kapasitas jaringan, laju data, dan cakupan dengan konsumsi daya rendah. Hal ini memerlukan perancangan antena yang sesuai untuk komunikasi nirkabel 5G agar mencapai bandwidth, radiasi, efisiensi, dan kinerja yang optimal. Desain antena MIMO menggunakan beberapa antena dan menghadapi tantangan utama dalam mengurangi mutual coupling antar elemen antena yang berdekatan. Dalam penelitian ini dirancang antena MIMO dengan menggunakan Teknik DGS T-Shaped dan elemen parasitic. Teknik DGS dikembangkan dengan membentuk suatu bidang pada bagian ground dari antena untuk meningkatkan kinerja antena. Untuk mencapai bandwidth besar dan gain yang tinggi, konsep DGS serta elemen parasitic dimasukkan ke dalam desain antena. Antena dirancang dengan dimensi sebesar 52mm x 12mm. Antena disimulasikan menggunakan software Ansys HFSS. Hasil pengukuran antena yang menggunakan bahan substrat Rogers Duroid RT5880 diperoleh nilai mutual coupling -54.2 dB, return loss -11.1 dB, Gain 13.11 dB, dan bandwidth yang cukup lebar. Sehingga antena yang diusulkan mampu bekerja pada frekuensi 28 GHz yang memenuhi kebutuhan aplikasi 5G.

**Kata kunci:** DGS, Elemen Parasitic, MIMO, Mutual Coupling, 5G

## I. INTRODUCTION

Telecommunications technology has reached the 5G generation, offering data speeds of at least 1 Gbps. The goal of 5G is to improve coverage, reduce power consumption, and enhance data rates and network capacity. Therefore, developing a suitable antenna for 5G communication is essential to achieve better performance, radiation efficiency, and increased bandwidth.

One cutting-edge technology known as multiple-input multiple-output (MIMO) uses multipath propagation by employing multiple antennas at both the transmitter and receiver [1]. Surface currents and waves, free space radiation, and mutual coupling all play a role in MIMO antennas [2]. As a result, limiting the mutual coupling relationship in antenna design is the primary obstacle in designing MIMO antennas.

Various methods can be used to reduce mutual coupling. In a comparative study, various methods were used, including DGS, Parasitic elements, EBG, decoupling and DRA [3]. The DGS method works to form a plane on the ground part of the antenna that can increase bandwidth. DGS produces -20dB mutual coupling at a frequency of 3-11GHz and produces a high gain of about 6 dB. The DRA method works to convert guided waves into unguided RF signals. DRA produces -18dB mutual coupling at a frequency of 6GHz and produces a gain of about 5 dB. Simple mutual coupling of -20dB at 11GHz and a high gain of about 8 dB are produced by parasitic elements working together on the patch [3]. The EBG method can block certain frequency electromagnetic waves, resulting in the mutual coupling of -18dB at a frequency of 2.48GHz and producing a gain of about 2.9dB. The decoupling method produces a gain of about 2dB [4]. Some of the shortcomings of the above method include EBG's complicated design, difficult fabrication, and difficult extraction parameters.

Some techniques to overcome limitations are mutual coupling, gain and lower bandwidth. The Defected Ground Structure (DGS) is the best method. This technique was developed by forming a plane on the ground part of the antenna to enhance the antenna's effectiveness. DGS serves as a resonant gap, facilitating the feed line-coupling efficiency. DGS also alters the distribution of shield currents on the ground plane in order to facilitate controlled electromagnetic excitation and propagation through substrates. This alters the capacitive and inductive responses of the transmission line. To put it another way, DGS raises capacitance and effective inductance, which results in much resonance and raises the antenna's bandwidth [5].

By increasing bandwidth and gain, suppressing higher levels of alignment, combining adjacent elements, and cross-polarizing, DGS is used to enhance the radiation characteristics of microstrip antennas [6]. The addition of parasitic elements can also increase the antenna gain. Several studies have been conducted regarding DGS techniques and parasitic elements. In [7], the use of DGS T-shaped and parasitic elements resulted in a Gain of 10.1 dB in 28 GHz–44 GHz. Research on the Trident-shaped UWB MIMO antenna in 2017. The method used is DGS T-shaped at a working frequency of 3.1-11.8 GHz. This study produced a Gain of 3.6-6 dBi [8].

In 2021, the research on a DGS-based T-shaped patch Antenna for use in 5G communication applications. At working frequencies of 30.30 and 35.1515 GHz, the method is DGS T-shaped. Gains of 17.66 and 13.75 dB were achieved in this study [9]. In 2021, the research on MIMO antenna isolation enhancement for millimeter wave applications. The technique is DGS T-shaped and operates between 20 and 28.6 GHz. A gain of 5 dBi [10] is obtained. The research in 2020 on a 28/38 GHz Dual-Band Microstrip Patch Antenna with DGS and Stub-Slot Configurations for 5G Wireless Communication. Stub slots and DGS are the two methods used. At 28 GHz, gains of 8.31 dB and at 38 GHz, gains of 6.38 dB [11].

Using parasitic elements and the DGS T-shaped technique with a 2-slot circular DGS, a MIMO antenna was created for this study. The T-shaped method was proposed in this study because it is easy in designing antennas. This design results in high gains and wide bandwidth on frequencies. To achieve large bandwidth and high gain, the concept of DGS, as well as parasitic elements, was incorporated into the antenna design. The Ansys HFSS software is used to simulate the antenna. The antenna design's outcomes have the potential to lessen the impact of mutual coupling, so that the proposed antenna can operate at 28 GHz, which is sufficient for 5G applications.

## II. ANTENNA DESIGN

### A. Determining the Antenna Parameters

The initial stage of antenna design is to determine the expected antenna characteristics, namely antenna working frequency, bandwidth impedance, return loss, mutual coupling, VSWR, and gain. As for the parameters of the desired antenna, as shown in Table 1.

Table 1. Antenna Parameters

Parameter	Antenna Charateristic
Frequency	28 GHz
Return Loss	< -10 dB
Mutual Coupling	< -20 dB
Gain	> 3 dB

In this case, the dimensions of the substrate used are:

Table 2. Dimensions Of The Substrate

Specification	Value
Type of Substrate	Rogers Duroid RT5880
Dielectric Constant	2,2
Thickness (h)	1,57 mm
Loss Tangent	0,0009

The Rogers Duroid RT5880 material was chosen because it has a low dielectric tangent loss value, which allows it to produce high gains and be used in high-frequency devices [12].

### B. T-Shaped Single Antenna Design with DGS and Parasitic Elements

The single antenna's design is T-shaped using DGS and parasitic elements, based on the calculation results of the antenna dimension formula. The dimensions are calculated based on a predetermined 28 GHz frequency and Rogers Duroid RT5880 substrate material. Fig 1 shows a single T-shaped antenna design using DGS and parasitic elements.

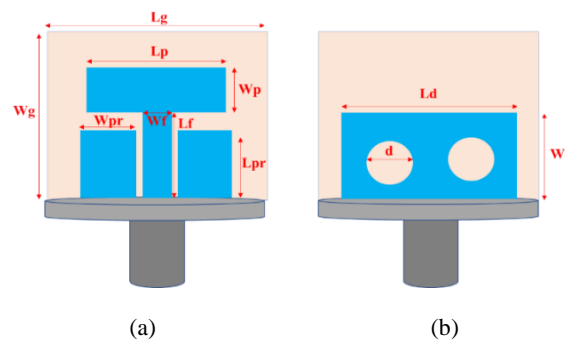


Fig. 1. Single T Shaped antennas with DGS and parasitic elements (a) Front View (b) Back View

Table 3 presents the parameters and simulation results based on the optimization outcomes. After optimizing the antenna parameters, the simulation results show significant improvement compared to the values obtained prior to optimization.

Table 3. Parameters Of Single T-Shaped Antenna With DGS And Parasitic Elements

Parameter	Symbol	Size (mm)
Width of Ground	$W_g$	12
Length of Ground	$L_g$	12
Width of Patch	$W_p$	2,9
Length of Patch	$L_p$	7,8
Width of Feedline	$W_f$	1,3
Height of Feedline	$L_f$	5,87
Width of ground DGS	$W_d$	5,7
Length of ground DGS	$L_d$	10
Diameter of Circular Slots	$D$	1,15
Height of parasitic	$L_{pr}$	4,55
Width of Parasitic	$W_{pr}$	3,2

### C. MIMO 2 Antenna Port 1-3

The design of MIMO 2 antenna ports 1-3 combines several elements of antenna justice, where the size is adjusted to the length and width of 52x12 mm. The MIMO design of 2 antenna ports 1-3 is shown in Figs 2 and 3. MIMO designed 2 antenna ports 1-3 using DGS and parasitic elements based on the optimization results of a single antenna. Figs 2 and 3 show the design of MIMO 2 antenna ports 1-3 with DGS and parasitic elements.

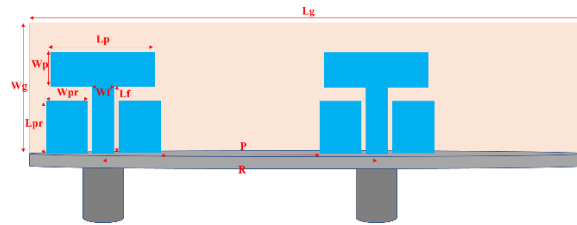


Fig. 2. MIMO 2 Antenna Ports 1-3 with DGS and Parasitic Elements (Front View)

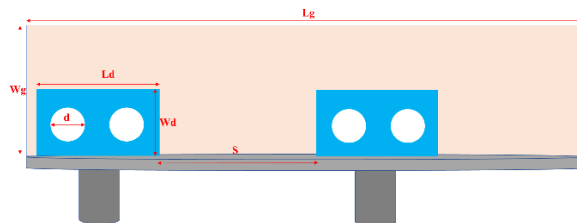


Fig 3. MIMO 2 Antenna Ports 1-3 with DGS and Parasitic Elements (Back View)

Table 4 presents the parameters and simulation results based on the optimization outcomes. After optimizing the antenna parameters, the simulation results show significant improvement compared to the values obtained prior to optimization.

Table 4. MIMO Parameters 2 Antenna Ports 1-3 With DGS And Parasitic Elements

Parameter	Symbol	Size (mm)
Width of Ground	$W_g$	12
Length of Ground	$L_g$	48
Width of Patch	$W_p$	2,9
Length of Patch	$L_p$	7,8

Width of Feedline	Wf	1,3
Height of Feedline	Lf	5,87
Width of ground DGS	Wd	5,7
Length of ground DGS	Ld	10
Diameter of Circular Slots	D	1,15
Height of parasitic	Lpr	4,55
Width of Parasitic	Wpr	3,2
Separation between two DGS	S	16
Separation between two antenna	R	26
Separation between two parasitic antenna	P	17,6

**D. MIMO 2 Antenna Port 1-4**

The design of MIMO 2 antenna ports 1-4 combines several elements of antenna justice, where the size is adjusted to the length and width of 52x12 mm. The MIMO design of 2 antenna ports 1-4 is shown in Figs 4 and 5. MIMO designed 2 antenna ports 1-4 using DGS and parasitic elements based on the optimization results of a single antenna. Figs 4 and 5 show the design of MIMO 2 antenna ports 1-4 by using DGS and parasitic elements.

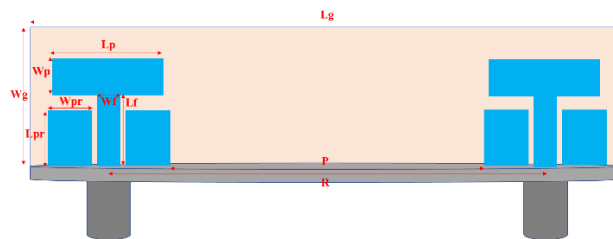


Fig. 4. MIMO 2 Antenna Ports 1-4 with DGS and Parasitic Elements (Front View)

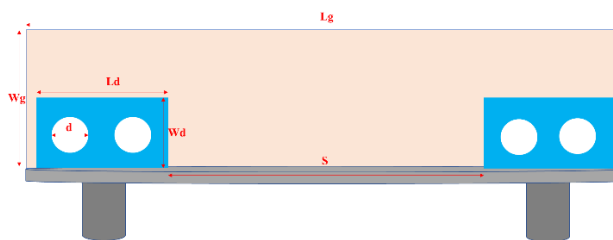


Fig. 5. MIMO 2 Antenna Ports 1-4 with DGS and Parasitic Elements (Back View)

Table 5 presents the parameters and simulation results based on the optimization outcomes. After optimizing the antenna parameters, the simulation results show significant improvement compared to the values obtained prior to optimization.

Table 5. MIMO Parameters 2 Antenna Ports 1-4 With DGS And Parasitic Elements

Parameter	Symbol	Size (mm)
Width of Ground	Wg	12
Length of Ground	Lg	48
Width of Patch	Wp	2,9
Length of Patch	Lp	7,8
Width of Feedline	Wf	1,3

Height of Feedline	Lf	5,87
Width of ground DGS	Wd	5,7
Length of ground DGS	Ld	10
Diameter of Circular Slots	D	1,15
Height of parasitic	Lpr	4,55
Width of Parasitic	Wpr	3,2
Separation between two DGS	S	29
Separation between two antenna	R	39
Separation between two parasitic antenna	P	30,6

### E. MIMO 4 Antenna

The MIMO with four antennas combines several elements of antenna justice, where the size is adjusted to the length and width of 52x12 mm. The design of the 4-antenna MIMO is shown in Figs 6 and 7. MIMO 4 antenna design using DGS and parasitic elements based on the optimization results of a single antenna. Figs 6 and 7 show the design of the MIMO 4 antenna by using DGS and parasitic elements.

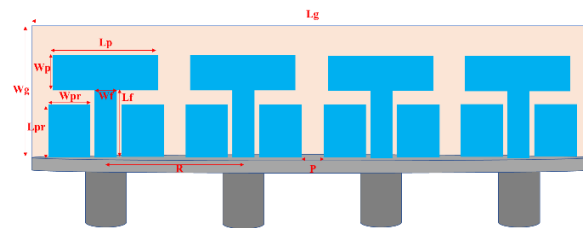


Fig. 6. MIMO 4 Antennas with DGS and Parasitic Elements (Front View)

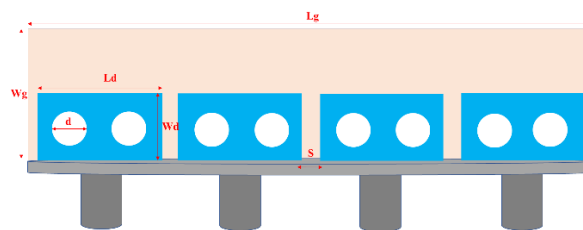


Fig. 7. MIMO 4 Antenna with DGS and Parasitic Elements (Back View)

Table 6 presents the parameters and simulation results based on the optimization outcomes. After optimizing the antenna parameters, the simulation results show significant improvement compared to the values obtained prior to optimization.

Table 6. MIMO Parameters 4 Antennas With DGS And Parasitic Elements

Parameter	Symbol	Size (mm)
Width of Ground	Wg	12
Length of Ground	Lg	52
Width of Patch	Wp	2,9
Length of Patch	Lp	7,8
Width of Feedline	Wf	1,3
Height of Feedline	Lf	5,87
Width of ground DGS	Wd	5,7
Length of ground DGS	Ld	10
Diameter of Circular Slots	D	1,15
Height of parasitic	Lpr	4,55

Width of Parasitic	W <sub>pr</sub>	3,2
Separation between two DGS	S	3
Separation between two antenna	R	13
Separation between two parasitic antenna	P	4,6

### III. RESULT AND DISCUSSION

#### A. Antenna Simulation Comparison Results

Antenna designs, both single and MIMO, are simulated using Ansys HFSS 15. Once the antenna is simulated and passed characterization and optimization, it will produce several parameter values, such as return loss, VSWR, bandwidth, and gain, as shown by a comparison chart of a single antenna and a MIMO antenna. Fig 8 shows a comparison chart of the results of the simulated return loss (S11) of a single antenna without DGS and parasitic elements, a single antenna without DGS, a single antenna without parasitic elements, a single antenna with DGS and parasitic elements, MIMO 2 antenna ports 1-3, MIMO 2 antenna ports 1-4 and MIMO 4 antennas. Fig 8 shows the antenna design using the DGS and parasitic elements produced the best return loss on MIMO 2 Antenna ports 1-3 of -36.5 dB.

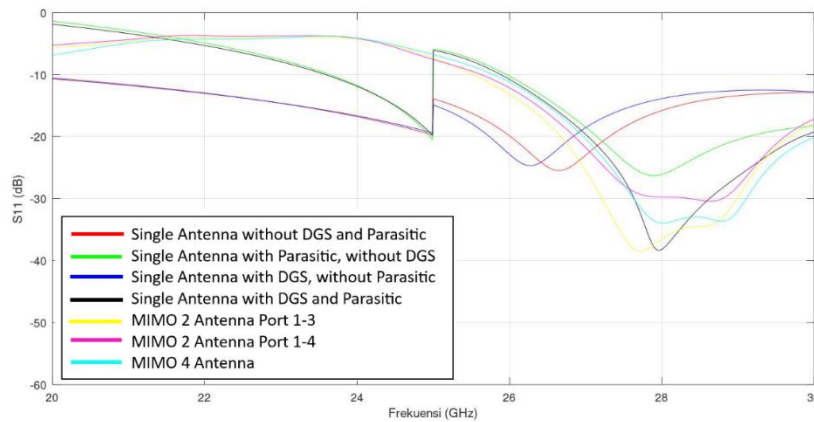


Fig. 8. Comparison of Return Loss Simulation Results on Single Antenna and MIMO

Table 7 shows the total gain values on single and MIMO antennas. The total gain value on the MIMO of 2 and 4 antennas is greater than that of the single antenna.

Table 7. Total Gain Simulation Table

Type	Antenna	28 GHz Frequency
		Gain (dB)
Single Antena T-Shaped without DGS & Parasitic	1 Antena	8,1
Single Antena with Parasitic, without DGS		6,9
Single Antena with DGS, without Parasitic		8,4
Single Antena T-Shaped with DGS & Parasitic		6,9
MIMO T-Shaped without DGS & Parasitic	4 Antena	14,3
MIMO with Parasitic, without DGS		13
MIMO with DGS, without Parasitic		14,3
MIMO T-Shaped with DGS & Parasitic		13,11
MIMO T-Shaped without DGS & Parasitic	2 Antena	11,6
MIMO T-Shaped with DGS & Parasitic (Port 1-3)		10,1
MIMO T-Shaped with DGS & Parasitic (Port 1-4)		9,8

## B. Comparison Results of MIMO Antenna Simulation and Measurement

After simulating both single antenna, MIMO 4 antenna and MIMO 2 antenna, the next step is to perform antenna fabrication using Rogers Duroid 5880 substrate material with a thickness of 1.57mm. After the antenna fabrication process is complete, a measurement process is carried out using the Vector Network Analyzer (VNA) tool. Fig 9 represents MIMO 2 antenna ports 1-3, MIMO antenna 4 antennas and MIMO 2 antenna ports 1-4 after the fabrication process. Fig 10 shows measurements on the MIMO 4 Antenna.



Fig. 9. Antennas After Fabrication



Fig. 10. MIMO Measurements of 4 Antennas

Fig 11 shows the results of a comparison of simulations and measurements of S11 on a MIMO 4 Antenna. In the simulation results, an S11 value of -33.9 dB and an S22 value of -34.6 dB were obtained. In the measurement results, an S11 value of -5.35 dB and an S22 value of -3.89 dB were obtained.



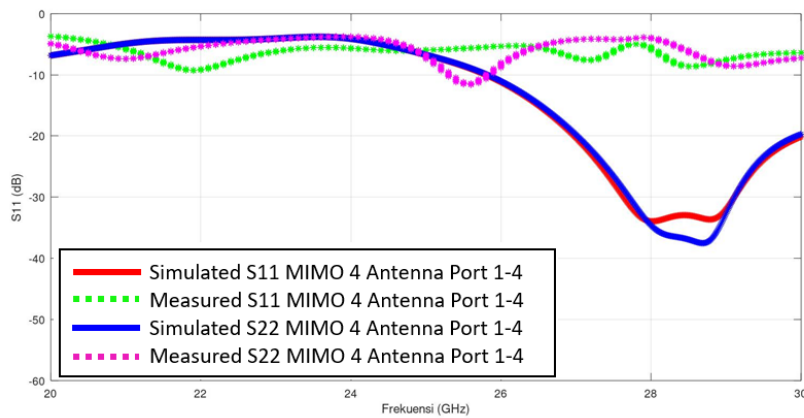


Fig. 11. Comparison Results of S11 Simulation and Measurement on a 4-Port MIMO Antenna

Fig 12 shows the results of a comparison of simulations and measurements of S21 on MIMO 4 Antennas. In the simulation results, an S21 value of -29 dB and an S12 value of -29 dB were obtained. In the measurement results, an S21 value of -54.2 dB and an S12 value of -54.4 dB were obtained.

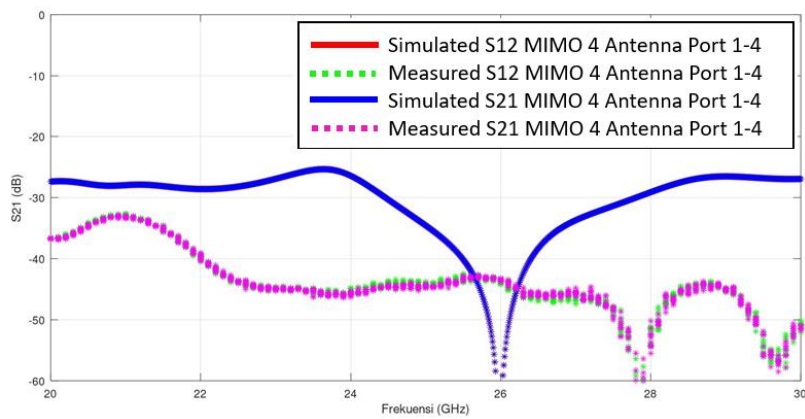


Fig. 12. Comparison Results of Simulation and Measurement of S21 on a 4-Port MIMO Antenna

Fig 13 shows measurements on MIMO 2 Antenna ports 1-3, where measurements on ports 1 and 3 on MIMO 2 Antenna are taken. The distance between the antennas is 26 mm. The ports connected to the VNA are Ports 1 and 3.



Fig. 13. MIMO Measurements 2 Antenna Ports 1-3

Fig 14 shows the results of a comparison of simulations and measurements of S11 on MIMO 2 Antenna Ports 1-3. In the simulation results, an S11 value of -36.5 dB and an S22 value of -30.9 dB were obtained. In contrast, the measurement results obtained an S11 value of -11.1 dB and an S22 value of -11.7 dB.

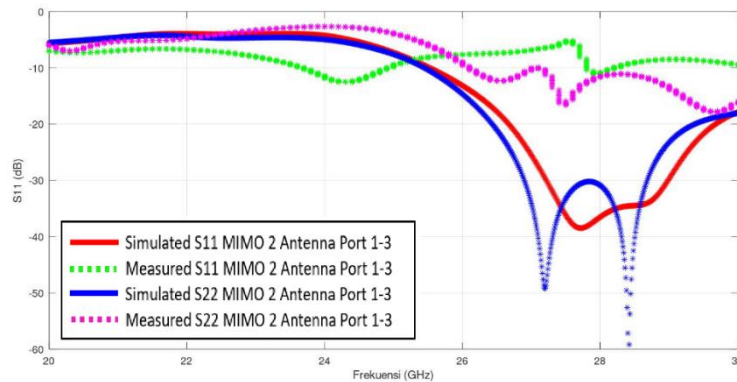


Fig. 14. Comparison Results of Simulation and Measurement of S11 on MIMO 2 Antenna Ports 1-3

Fig 15 shows the results of a comparison of simulations and measurements of S21 on MIMO 2 Antenna Ports 1-3. In the simulation results, an S21 value of -26.5 dB and an S12 value of -26.5 dB were obtained. Meanwhile, the measurement results obtained an S21 value of -41.6 dB and an S12 value of -42.2 dB.

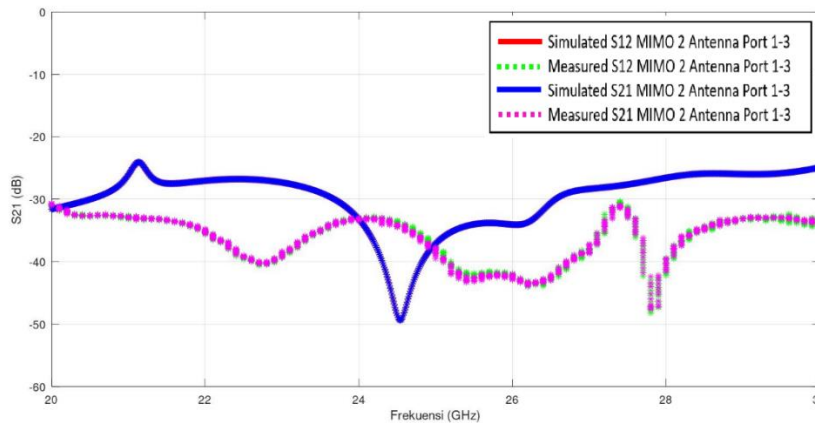


Fig. 15. Comparison Results of Simulation and Measurement of S21 on MIMO 2 Antenna Ports 1-3

Fig 16 shows measurements on MIMO 2 Antenna ports 1-4 where measurements on ports 1 and 4 on MIMO 2 Antenna. The distance between the antennas is 39 mm. The ports connected to the VNA are Ports 1 and 4.



Fig. 16. MIMO Measurements 2 Antenna Ports 1-4

Fig 17 shows the results of a comparison of simulations and measurements of S11 on MIMO 2 Antenna Ports 1-4. In the simulation results, an S11 value of -29.7 dB and an S22 value of -33.2 dB were obtained. Meanwhile, the measurement results obtained an S11 value of -4.69 dB and an S22 value of -4.42 dB.

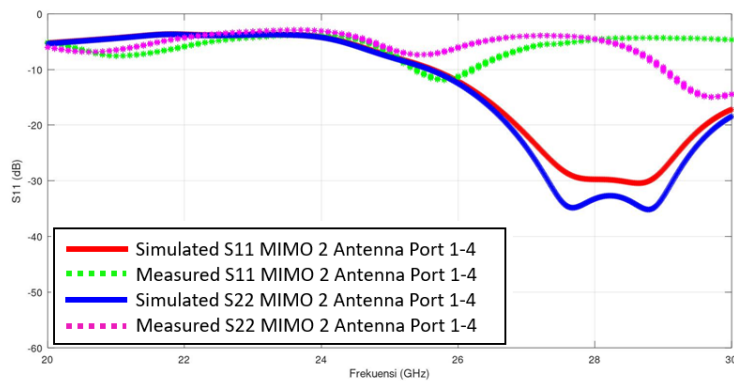


Fig. 17. Comparison Results of Simulation and Measurement of S11 on MIMO 2 Antenna Ports 1-4

Fig 18 shows the results of a comparison of simulations and measurements of S21 on MIMO 2 Antenna Ports 1-4. In the simulation results, an S21 value of -28.8 dB and an S12 value of -28.8 dB were obtained. At the same time, the measurement results obtained an S21 value of -50 dB and an S12 value of -49.5 dB.

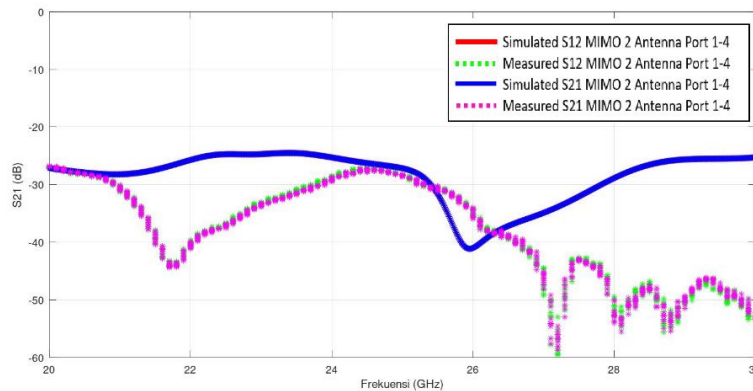


Fig. 18. Comparison Results of S21 Simulation and Measurement on MIMO 2 Antenna Ports 1-4

#### IV. CONCLUSIONS

This research using the DGS and parasitic elements method has the advantage of reducing the mutual coupling effect of the antenna and improving antenna performance in 5G applications. This is evidenced by the comparison between the simulation results and measurements on the MIMO 4 antennas, MIMO 2 antennas ports 1-3 and MIMO 2 antennas ports 1-4. Obtained the best S11 measurement value on MIMO 2 antenna ports 1-3, which is -11.1 dB, and the best S21 measurement value on MIMO 4 antennas is -54.2 dB. The DGS and Parasitic Elements methods on the MIMO antenna also affect the increase in antenna gain and bandwidth expansion. Furthermore, this was proven in this research, where the design of the MIMO antenna obtained a gain of 13.11 dB when compared to a single antenna microstrip antenna which only produced a gain of 6.9 dB. There was an increase in gain of 6.21 dB.

#### REFERENCES

- [1] U. Ullah, I. Ben Mabrouk, S. Koziel, M. Al-Hasan and R. Shubair. "An Ultra-Wideband Circularly Polarized Multiple-Input Multiple-Output Antenna with Polarization Diversity," 2019 International Conference on Electrical and Computing Technologies and Applications (ICECTA). 2019. pp. 1-3, doi: 10.1109/ICECTA48151.2019.8959558.
- [2] Zhang, Y. M., & Zhang, S. A Side-Loaded-Metal Decoupling Method for  $2 \times N$  Patch Antenna Arrays. *IEEE Antennas and Wireless Propagation Letters*, 2021. 20(5), 668-672.
- [3] Nadeem, I., & Choi, D. Y. Study on mutual coupling reduction technique for MIMO antennas. *IEEE Access*, 2019. 7, 563-586.
- [4] Chen, X., Zhang, S., & Li, Q. A review of mutual coupling in MIMO systems. *IEEE Access*, 2018. 6, 24706-24719.
- [5] Koesmarijanto, K., Alifia, N. A. P., & Darmono, H. Design and Implementation of  $2 \times 4$  Element Hexagonal Array Microstrip Antenna with DGS Method in the Shape of Dumbbell Circle Head for 2.4 GHz Frequency Wi-Fi Applications. *Journal of Telecommunication Network (Jurnal Jaringan Telekomunikasi)*, 2022. 12(4), 232-238.
- [6] Khandelwal, M. K., Kanaujia, B. K., & Kumar, S. Defected ground structure: fundamentals, analysis, and applications in modern wireless trends. *International Journal of Antennas and Propagation*, 2017(1), 2018527.
- [7] Rao, P. K., Chaurasia, R., Verma, R., Gupta, H., Pathak, S., & Mishra, R. T-Shape MIMO Antenna with Parasitic Element and DGS for 5G Applications. *Journal of Telecommunication, Electronic and Computer Engineering (JTECE)*, 2021. 13(3), 7-11.
- [8] Jetti, C. R., & Nandanavanam, V. R. Trident-shape strip loaded dual band-notched UWB MIMO antenna for portable device applications. *AEU-International Journal of Electronics and Communications*, 83, 2018. 11-21.
- [9] Gupta, A. K., Patnaik, A. K., Suresh, S., Chowdary, P. S. R., & Krishna, M. V. DGS-Based T-Shaped Patch Antenna for 5G Communication Applications. In *Microelectronics, Electromagnetics and Telecommunications*, 2021. (pp. 11-19). Springer, Singapore.
- [10] Singh, S. V., Pratap, J., Singh, A., Sharma, S., & Gupta, S. Isolation Enhancement of MIMO Antenna for Millimeter wave Applications. In 2021 2nd International Conference on Intelligent Engineering and Management (ICIEM), 2021. (pp. 466-470). IEEE.
- [11] Hakim, M. L., Uddin, M. J., & Hoque, M. J. 28/38 GHz Dual-Band Microstrip Patch Antenna with DGS and Stub-Slot Configurations and Its  $2 \times 2$  MIMO Antenna Design for 5G Wireless Communication. In 2020 IEEE Region 10 Symposium (TENSymp), 2020. (pp. 56-59). IEEE.
- [12] Preethi, V., Swamalatha, P., Rajpoot, V., Krishna, R. V. V., & Kumar, S. Design and Implementation of Circular Microstrip Patch Array Antenna for 5G Communication Using Rogers RT5880. In 2023 International Conference on Advanced & Global Engineering Challenges (AGEC), 2023. (pp. 32-37). IEEE.

- [13] L. Ammai, R. Anwar, and D. A. Nurmantris. "Analysis on multi rings defected ground structure for microstrip antenna miniaturization," in 2017 International Conference on Engineering Technology and Technopreneurship (ICE2T). IEEE, 2017, pp. 1–4.
- [14] Ping Dong, Tao Zheng, Shui Yu, Hongke Zhang and Xiaoyun Yan. Enhancing Vehicular Communication Using 5G-enabled Smart Collaborative Networking. *IEEE Wireless Communications*, 24(6), 2017. 72-79.
- [15] P. K. Rao and R. Mishra. Multi Band Antenna with Multi Band Notch 2.5/3.7/6.4/8.1/12.4/14.4GHz Characteristics. 5th IEEE Uttar Pradesh Section International Conference on Electrical, Electronics and Computer Engineering (UPCON), Gorakhpur, 2018, pp. 1-5, doi: 10.1109/UPCON.2018.8596938
- [16] Khattak, R. Y., Shoaib, S., Shah, R. A., & Hussain, A. Design and Performance Investigation of Array Antenna for 60 GHz WiGig Terminals. In *2021 IEEE Conference of Russian Young Researchers in Electrical and Electronic Engineering (ElConRus), 2021*. pp. 2521-2524.
- [17] A. Ghalib and M. S. Sharawi, "TCM Analysis of Defected Ground Structures for MIMO Antenna Designs in Mobile Terminals," in *IEEE Access*, vol. 5, 2017. pp. 19680-19692, doi: 10.1109/ACCESS.2017.2739419.